



Syntheses and structures of ammonium transition-metal dialuminium tris(phosphate) dihydrates $(\text{NH}_4)\text{MAl}_2(\text{PO}_4)_3 \cdot 2\text{H}_2\text{O}$ ($M = \text{Mn}$ and Ni)

Makoto Tokuda,* Keita Tanaka and Kazumasa Sugiyama

Institute for Materials Research, Tohoku University, 2-1-1 Katahira, Aoba-ku, Sendai 980-8577, Japan. *Correspondence e-mail: makoto.tokuda.b7@tohoku.ac.jp

Received 20 July 2022
Accepted 23 January 2023

Edited by W. T. A. Harrison, University of Aberdeen, United Kingdom

Keywords: single-crystal diffraction; crystal structure; aluminophosphate.

CCDC references: 2237562; 2237561

Supporting information: this article has supporting information at journals.iucr.org/e

The structures of ammonium manganese(II) dialuminium tris(phosphate) dihydrate, $(\text{NH}_4)\text{MnAl}_2(\text{PO}_4)_3 \cdot 2\text{H}_2\text{O}$, and ammonium nickel(II) dialuminium tris(phosphate) dihydrate, $(\text{NH}_4)\text{NiAl}_2(\text{PO}_4)_3 \cdot 2\text{H}_2\text{O}$, were determined using single-crystal diffraction data. The structures of title compounds are isotypic to cobalt aluminophosphate, $(\text{NH}_4)\text{CoAl}_2(\text{PO}_4)_3 \cdot 2\text{H}_2\text{O}$ (LMU-3) [Panz *et al.* (1998). *Inorg. Chim. Acta*, **269**, 73–82], in which a three-dimensional network of vertex-sharing AlO_5 and PO_4 moieties delineate twelve-membered channels in which ammonium, NH_4^+ , and transition-metal cations ($M = \text{Mn}^{2+}$ and Ni^{2+}) reside as charge compensators for the anionic $[\text{Al}_2(\text{PO}_4)_3]^{3-}$ aluminophosphate framework. In both structures, the N atom of the ammonium cation, the transition-metal ion and one of the P atoms lie on crystallographic twofold axes.

1. Chemical context

The mixed-metal phosphate composed of tetrahedral, bipyramidal and octahedral building units with chemical formula $\text{KNiAl}_2(\text{PO}_4)_3 \cdot 2\text{H}_2\text{O}$ was firstly reported by Meyer & Haushalter (1994). Isotypic structures were found in the aluminophosphates; $(\text{NH}_4)\text{CoAl}_2(\text{PO}_4)_3 \cdot 2\text{H}_2\text{O}$ (Panz *et al.* 1998), $\text{KMnAl}_2(\text{PO}_4)_3 \cdot 2\text{H}_2\text{O}$ (Kiriukhina *et al.* 2020), $\text{CsFe}_3(\text{PO}_4)_3 \cdot 2\text{H}_2\text{O}$ (Lii & Huang 1995), $(\text{NH}_4)\text{CoGa}_2(\text{PO}_4)_3 \cdot 2\text{H}_2\text{O}$ (Chippindale *et al.* 1996), $(\text{NH}_4)\text{MnGa}_2(\text{PO}_4)_3 \cdot 2\text{H}_2\text{O}$ (Chippindale *et al.* 1998), $(\text{NH}_4)\text{NiGa}_2(\text{PO}_4)_3 \cdot 2\text{H}_2\text{O}$ (Bieniek *et al.* 2008) and $\text{KNiGa}_2(\text{PO}_4)_3 \cdot 2\text{H}_2\text{O}$ (Chippindale *et al.* 2009).

Herein, we report the syntheses and structures of $(\text{NH}_4)\text{MAl}_2(\text{PO}_4)_3 \cdot 2\text{H}_2\text{O}$ [$M = \text{Mn}$ in (I) and Ni in (II)] using a hydrothermal technique and structural analysis by single-crystal X-ray diffraction. These compounds are isotypic to $(\text{NH}_4)\text{CoAl}_2(\text{PO}_4)_3 \cdot 2\text{H}_2\text{O}$ (LMU-3), crystallizing from a hydrothermal synthesis (Panz *et al.*, 1998).

2. Structural commentary

The aluminophosphate framework of the title compounds with the chemical formula $(\text{NH}_4)\text{MAl}_2(\text{PO}_4)_3 \cdot 2\text{H}_2\text{O}$ ($M = \text{Mn}$ and Ni) is composed of $[\text{PO}_4]$ tetrahedra and $[\text{AlO}_5]$ trigonal-bipyramids. Fig. 1(a) shows the $[\text{Al}_2(\text{PO}_4)_3]_\infty$ layers, which are built up from four- and eight-membered rings connected *via* $\text{Al}-\text{O}-\text{P}$ bonds. These layers stack along the a -axis direction, with the $[\text{P}_2\text{O}_4]$ tetrahedra (atom P2 lies on a crystallographic twofold axis) bridging between them, leading to the formation of a three-dimensional network encapsulating twelve-membered channels propagating in the $[001]$ direction. The

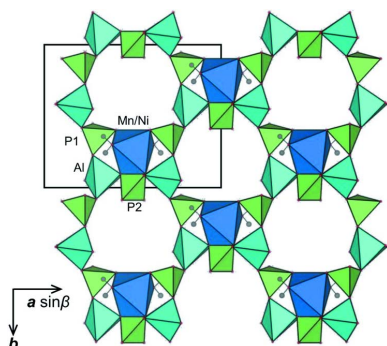


Table 1

 Selected bond lengths (Å) in $(\text{NH}_4)\text{MAl}_2(\text{PO}_4)_3 \cdot 2\text{H}_2\text{O}$ [$M = \text{Mn}$ (I) and Ni (II)].

	(I)	(II)
<i>PO₄ tetrahedra</i>		
P1–O6 ^{iv}	1.5152 (19)	1.5180 (14)
P1–O2	1.5342 (19)	1.5361 (14)
P1–O3	1.5350 (18)	1.5371 (13)
P1–O1	1.5493 (18)	1.5502 (13)
P2–O5	1.5294 (18)	1.5253 (13)
P2–O4	1.5420 (18)	1.5444 (13)
<i>AlO₅ trigonal bipyramid</i>		
Al–O2 ⁱⁱ	1.7847 (19)	1.7731 (14)
Al–O1	1.8013 (19)	1.7908 (14)
Al–O5 ^{iv}	1.8080 (18)	1.7979 (14)
Al–O3 ^{iv}	1.8886 (19)	1.8818 (14)
Al–O4	1.9320 (18)	1.9271 (14)
<i>MnO₆ octahedra</i>		
M–O6	2.0799 (19)	2.0052 (13)
M–O7	2.1990 (20)	2.0799 (15)
M–O4	2.2805 (18)	2.1512 (13)
O4···O4 ⁱ	2.407 (5)	2.387 (4)
O6···O7	2.950 (3)	2.785 (2)
O6···O7 ⁱ	2.962 (4)	2.844 (3)
O4···O6	3.192 (3)	3.065 (2)
O4···O7	3.254 (3)	3.089 (2)
O4···O7 ⁱ	3.291 (3)	3.094 (3)
O6···O6 ⁱ	3.372 (5)	3.132 (4)

 Symmetry codes: (i) $-x, y, -z + \frac{1}{2}$; (ii) $-x + \frac{1}{2}, y - \frac{1}{2}, -z + \frac{1}{2}$; (iv) $x, -y + 1, z - \frac{1}{2}$; (vi) $-x + \frac{1}{2}, y + \frac{1}{2}, -z + 1$.

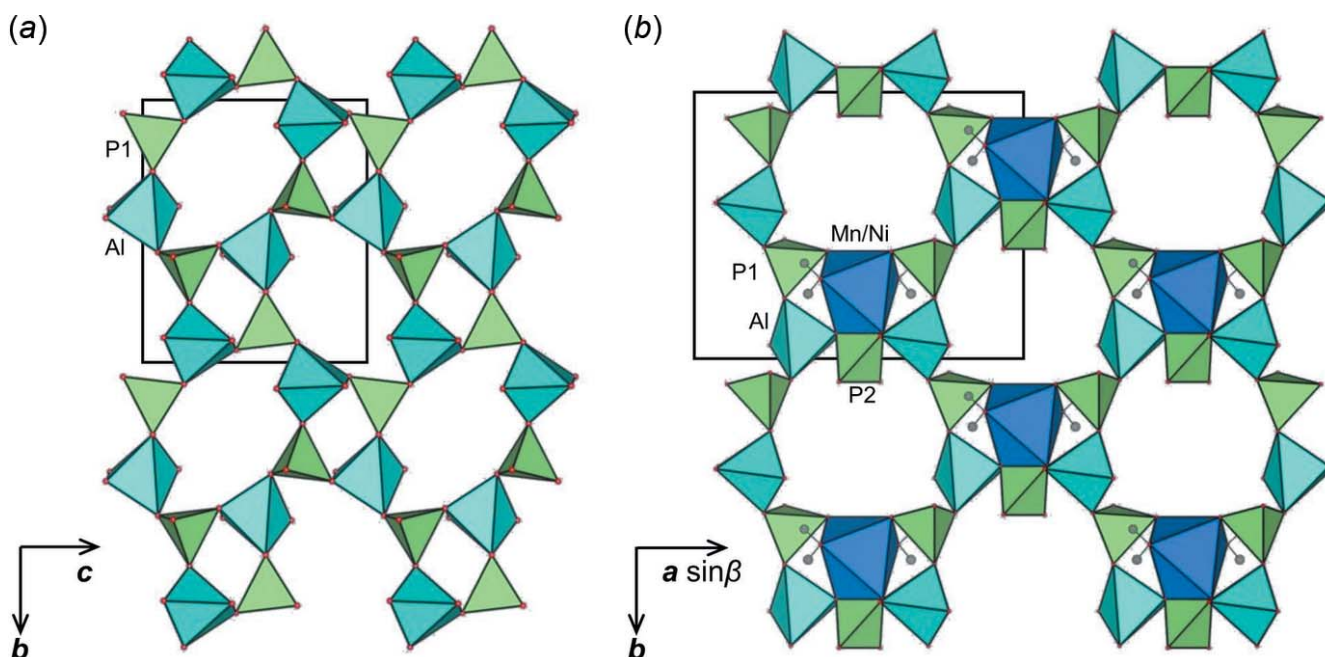
ammonium and transition-metal cations are respectively located in and on these channels, compensating the negative charge of the aluminophosphate framework [Fig. 1(b)].

There are two axial and three equatorial Al–O bonds within the $[\text{AlO}_5]$ trigonal bipyramids (Table 1). The axial

Al–O bond distances for $M = \text{Mn}$ are 1.8886 (19) and 1.9320 (18) Å and those for Ni are 1.8818 (14) and 1.9271 (14) Å, and the equatorial ones are in the ranges 1.7847 (19)–1.8080 (18) Å (Mn) and 1.7731 (14)–1.7979 (14) Å (Ni), thus the average axial Al–O bond distances are larger than the equatorial ones. Previous studies on $[\text{AlO}_5]$ trigonal bipyramids in LMU-3, $\text{KNiAl}_2(\text{PO}_4)_3 \cdot 2\text{H}_2\text{O}$, $\text{KMnAl}_2(\text{PO}_4)_3 \cdot 2\text{H}_2\text{O}$ and $(\text{NH}_4)_3\text{Al}_2(\text{PO}_4)_3$ (Panz *et al.*, 1998; Meyer & Haushalter 1994; Kiriukhina *et al.*, 2020; Medina *et al.* 2004) showed similar geometrical features with longer axial Al–O bonds distances.

The transition-metal cations, which lie on crystallographic twofold axes, are octahedrally coordinated by two oxygen atoms of water molecules and four oxygen atoms of the framework (Fig. 2). The mean M –O bond distances for the Mn and Ni compounds are 2.186 Å and 2.079 Å, respectively, which are consistent with the ionic radii of $^{\text{VI}}\text{Mn}^{2+}$ (0.83 Å) and $^{\text{VI}}\text{Ni}^{2+}$ (0.69 Å; Shannon 1976). The MO_6 octahedron shares an edge $\text{O4} \cdots \text{O4}$ with the adjacent $[\text{P2O}_4]$ tetrahedron. The length of the shared-edge $\text{O4} \cdots \text{O4}$ is the shortest among the twelve edges of octahedrally coordinated transition-metal cations in accordance with the P^{5+} – M^{2+} cation repulsion (Pauling, 1929, 1960).

The positions of the hydrogen atoms in the water molecule, H71 and H72, could be determined by analysing the residual peaks in the difference-Fourier maps. The oxygen atom O7 of the water molecule is coordinated to the transition-metal ions, and hydrogen atoms of H71 and H72 form $\text{O} \cdots \text{H} \cdots \text{O}$ hydrogen bonds with the oxygen atoms O1 and O3 of the $[\text{Al}_2(\text{PO}_4)_3]_\infty$ layer, respectively (Tables 2 and 3). Thus, the $\text{H71} \cdots \text{O1}$ and $\text{H72} \cdots \text{O3}$ hydrogen bonds contribute to the accumulation of the layers.


Figure 1

(a) Two-dimensional layer formed by four- and eight-membered rings in the bc plane and (b) the three-dimensional channels formed by twelve-membered rings in the aluminophosphate framework of $\text{Al}_2\text{M}(\text{NH}_4)(\text{PO}_4)_3 \cdot 2\text{H}_2\text{O}$ ($M = \text{Mn}$ and Ni) illustrated using VESTA (Momma & Izumi, 2011).

Table 2
Hydrogen-bond geometry (Å, °) for (I).

$D-H\cdots A$	$D-H$	$H\cdots A$	$D\cdots A$	$D-H\cdots A$
$O7-H71\cdots O1^i$	0.89	1.95	2.831 (3)	178
$O7-H72\cdots O3^{ii}$	0.87	2.04	2.897 (3)	166

Symmetry codes: (i) $x, -y + 1, z + \frac{1}{2}$; (ii) $-x + \frac{1}{2}, -y + \frac{1}{2}, -z + 1$.

As for the hydrogen-bonding interactions of the ammonium cation (N atom site symmetry 2) within the title compounds, not all the H atoms could be definitively located from difference maps but some structural information could be obtained from the observed distances $N1\cdots O5 = 3.085$ (5) and 3.103 (4) Å and $N1\cdots O6 = 2.906$ (4) and 2.862 (3) Å for

Table 3
Hydrogen-bond geometry (Å, °) for (II).

$D-H\cdots A$	$D-H$	$H\cdots A$	$D\cdots A$	$D-H\cdots A$
$O7-H71\cdots O1^i$	0.81	1.99	2.790 (2)	167
$O7-H72\cdots O3^{ii}$	0.86	2.11	2.961 (2)	170

Symmetry codes: (i) $x, -y + 1, z + \frac{1}{2}$; (ii) $-x + \frac{1}{2}, -y + \frac{1}{2}, -z + 1$.

$(NH_4)MAl_2(PO_4)_3\cdot 2H_2O$ ($M = Mn$ and Ni), respectively. The longer $N1\cdots O5$ distance and the large isotropic atomic displacement parameters, U_{iso} , of the N1 atom clearly indicate the relatively weaker hydrogen bonding for the presumed $N1-H\cdots O5$ cases. This structural feature did not allow us to definitively locate the positions of hydrogen atoms within the $N1-H\cdots O5$ cases. Nevertheless, some of the hydrogen-atom positions around the ammonium cations could be located in the difference-Fourier maps and coordinates are (0.5382, 0.3998, 0.2391) and (0.5357, 0.4204, 0.2296) for $(NH_4)MAl_2(PO_4)_3\cdot 2H_2O$ ($M = Mn$ and Ni), respectively. These possible hydrogen-atom positions correspond to those for the $N1-H\cdots O6$ cases. Weak hydrogen bonds between NH_4^+ and the framework suggests that NH_4^+ and a monovalent cation (e.g., alkali cation or H_3O^+) are exchangeable akin to zeolitic cations in this unique framework structure (Meyer & Haushalter 1994; Kiriukhina *et al.*, 2020). The chemical formula for the group of compounds reported in this study can be denoted by $A^+M^{2+}Al_2(PO_4)_3\cdot 2H_2O$ ($A =$ monovalent cation, $M =$ divalent transition-metal cation).

3. Synthesis and crystallization

Single crystals of $(NH_4)MAl_2(PO_4)_3\cdot 2H_2O$ ($M = Mn$ and Ni) were obtained as by-products of the laumontite-type zeolite imidazole-templated hydrothermal technique. The precursor solution was prepared by dissolving the chemical agents of imidazole, aluminium-isopropoxide and H_3PO_4 (85% solution): the transition-metal component (Ni or Mn) was added to the solution. For the insertion of nickel in the system, $(CH_3COO)_2Ni\cdot 4H_2O$ was used and for corresponding manganese analogue $(CH_3COO)_2Mn\cdot 4H_2O$ was added to the as-prepared precursor solution. In each case, the resultant gel mixture was then sealed in a Teflon-lined tube and heated at 453 K for three days.

A few colorless, transparent crystals of $(NH_4)MnAl_2(PO_4)_3\cdot 2H_2O$ with a plate-like form were separated from the microcrystalline material together with the laumontite-type aluminophosphate, Mn-hureaulite $Mn_5[PO_3(OH)]_2(PO_4)_2\cdot 4H_2O$. In the case of Ni, the product comprises $NH_4NiAl_2(PO_4)_3\cdot 2H_2O$, which forms colorless, transparent plate-like crystals and organic compounds.

The chemical analyses of the synthesized products were performed using energy-dispersive X-ray spectroscopy (EDS). The EDS profile clearly showed the presence of nitrogen. This supports the idea that NH_4^+ , a decomposition product of imidazole, was incorporated within the framework as a charge-compensating cation.

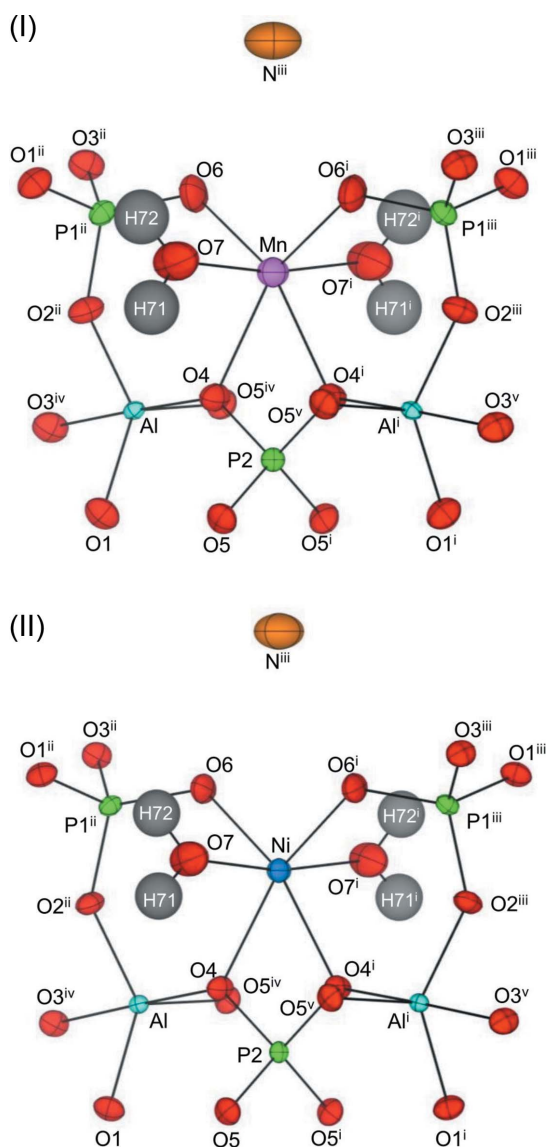


Figure 2
Positions of the MO_6 [$M = Mn$ (I) and Ni (II)] octahedra in the twelve-membered-ring channel of the aluminophosphate framework. Displacement ellipsoids are presented at the 80% probability level. [Symmetry codes: (i) $-x, y, -z + \frac{1}{2}$; (ii) $-x + \frac{1}{2}, y - \frac{1}{2}, -z + \frac{1}{2}$; (iii) $x - \frac{1}{2}, y - \frac{1}{2}, z$; (iv) $x, -y + 1, z - \frac{1}{2}$; (v) $-x, -y + 1, -z + 1$.]

Table 4
Experimental details.

	(NH ₄)MnAl ₂ (PO ₄) ₃ ·2H ₂ O	(NH ₄)NiAl ₂ (PO ₄) ₃ ·2H ₂ O
Crystal data		
M_r	447.88	451.65
Crystal system, space group	Monoclinic, <i>C2/c</i>	Monoclinic, <i>C2/c</i>
Temperature (K)	298	298
a, b, c (Å)	13.3577 (7), 10.2279 (5), 8.7922 (5)	13.0711 (3), 10.1772 (2), 8.74476 (19)
β (°)	108.885 (6)	108.527 (3)
V (Å ³)	1136.53 (11)	1103.00 (4)
Z	4	4
Radiation type	Mo $K\alpha$	Mo $K\alpha$
μ (mm ⁻¹)	1.85	2.44
Crystal size (mm)	0.05 × 0.04 × 0.02	0.11 × 0.04 × 0.03
Data collection		
Diffractometer	XtaLAB Synergy, Single source at offset/far, HyPix	XtaLAB Synergy, Single source at offset/far, HyPix
Absorption correction	Numerical (<i>CrysAlis PRO</i> ; Rigaku OD, 2021)	Numerical (<i>CrysAlis PRO</i> ; Rigaku OD, 2021)
T_{\min}, T_{\max}	0.938, 0.968	0.853, 0.962
No. of measured, independent and observed [$I > 2\sigma(I)$] reflections	5256, 1316, 1178	9320, 1328, 1281
R_{int}	0.027	0.021
$(\sin \theta/\lambda)_{\text{max}}$ (Å ⁻¹)	0.653	0.660
Refinement		
$R[F^2 > 2\sigma(F^2)], wR(F^2), S$	0.027, 0.077, 1.11	0.018, 0.056, 1.14
No. of reflections	1316	1328
No. of parameters	97	97
H-atom treatment	H-atom parameters constrained	H-atom parameters constrained
$\Delta\rho_{\text{max}}, \Delta\rho_{\text{min}}$ (e Å ⁻³)	0.90, -0.51	0.42, -0.36

Computer programs: *CrysAlis PRO* 1.171.40.43a (Rigaku OD, 2021), *SHELXT2014/5* (Sheldrick, 2015a), *SHELXL2016/6* (Sheldrick, 2015b) and *VESTA* (Momma & Izumi, 2011).

4. Refinement details

The crystal data, data collection methods, and structure refinement details are summarized in Table 4. The positions of the hydrogen atoms bonded to O7 were estimated using the residual peaks in the difference Fourier maps and refined using a riding model. The U_{iso} parameters for hydrogen atoms were fixed at $1.5 \times$ the U_{iso} of O7.

Funding information

This work was supported financially by Grant-in-Aid for Scientific Research on Innovative Areas No. 18H05456.

References

Bieniok, A., Brendel, U., Lottermoser, W. & Amthauer, G. (2008). *Z. Kristallogr.* **223**, 186–194.
 Chippindale, A. M., Cowley, A. R. & Bond, A. D. (1998). *Acta Cryst. C* **54**, IUC9800061.
 Chippindale, A. M., Cowley, A. R. & Walton, R. I. (1996). *J. Mater. Chem.* **6**, 611–614.

Chippindale, A. M., Sharma, A. V. & Hibble, S. J. (2009). *Acta Cryst. E* **65**, i38–i39.
 Kiriukhina, G. V., Yakubovich, O. V., Shvanskaya, L. V., Kochetkova, E. M., Dimitrova, O. V., Volkov, A. S. & Simonov, S. V. (2020). *Acta Cryst. C* **76**, 302–310.
 Lii, K.-H. & Huang, C.-Y. (1995). *J. Chem. Soc. Dalton Trans.* pp. 571–574.
 Medina, M. E., Iglesias, M., Gutiérrez-Puebla, E. & Monge, M. A. (2004). *J. Mater. Chem.* **14**, 845–850.
 Meyer, L. M. & Haushalter, R. C. (1994). *Chem. Mater.* **6**, 349–350.
 Momma, K. & Izumi, F. (2011). *J. Appl. Cryst.* **44**, 1272–1276.
 Panz, C., Polborn, K. & Behrens, P. (1998). *Inorg. Chim. Acta*, **269**, 73–82.
 Pauling, L. (1929). *J. Am. Chem. Soc.* **51**, 1010–1026.
 Pauling, L. (1960). *The Nature of the Chemical Bond*, 3rd ed., p. 93. Ithaca: Cornell University Press.
 Rigaku OD (2021). *CrysAlis PRO*. Rigaku Oxford Diffraction, Yarnton, England.
 Shannon, R. D. (1976). *Acta Cryst. A* **32**, 751–767.
 Sheldrick, G. M. (2015a). *Acta Cryst. A* **71**, 3–8.
 Sheldrick, G. M. (2015b). *Acta Cryst. C* **71**, 3–8.

supporting information

Acta Cryst. (2023). E79, 116-119 [https://doi.org/10.1107/S2056989023000555]

Syntheses and structures of ammonium transition-metal dialuminium tris-(phosphate) dihydrates $(\text{NH}_4)\text{MAl}_2(\text{PO}_4)_3 \cdot 2\text{H}_2\text{O}$ ($M = \text{Mn}$ and Ni)

Makoto Tokuda, Keita Tanaka and Kazumasa Sugiyama

Computing details

For both structures, data collection: *CrysAlis PRO* 1.171.40.43a (Rigaku OD, 2021); cell refinement: *CrysAlis PRO* 1.171.40.43a (Rigaku OD, 2021); data reduction: *CrysAlis PRO* 1.171.40.43a (Rigaku OD, 2021); program(s) used to solve structure: *SHELXT2014/5* (Sheldrick, 2015a); program(s) used to refine structure: *SHELXL2016/6* (Sheldrick, 2015b).

Ammonium manganese(II) dialuminium tris(phosphate) dihydrate (I)

Crystal data

$(\text{NH}_4)\text{MnAl}_2(\text{PO}_4)_3 \cdot 2\text{H}_2\text{O}$

$M_r = 447.88$

Monoclinic, $C2/c$

$a = 13.3577$ (7) Å

$b = 10.2279$ (5) Å

$c = 8.7922$ (5) Å

$\beta = 108.885$ (6)°

$V = 1136.53$ (11) Å³

$Z = 4$

$F(000) = 956.0$

$D_x = 2.618$ Mg m⁻³

Mo $K\alpha$ radiation, $\lambda = 0.71073$ Å

Cell parameters from 3620 reflections

$\theta = 3.9\text{--}27.6^\circ$

$\mu = 1.85$ mm⁻¹

$T = 298$ K

Plate, colourless

$0.05 \times 0.04 \times 0.02$ mm

Data collection

XtaLAB Synergy, Single source at offset/far,

HyPix

diffractometer

Radiation source: micro-focus sealed X-ray

tube, PhotonJet (Mo) X-ray Source

Mirror monochromator

Detector resolution: 10.0000 pixels mm⁻¹

ω scans

Absorption correction: numerical

(CrysAlisPro; Rigaku OD, 2021)

$T_{\min} = 0.938$, $T_{\max} = 0.968$

5256 measured reflections

1316 independent reflections

1178 reflections with $I > 2\sigma(I)$

$R_{\text{int}} = 0.027$

$\theta_{\max} = 27.6^\circ$, $\theta_{\min} = 3.2^\circ$

$h = -17 \rightarrow 17$

$k = -13 \rightarrow 11$

$l = -11 \rightarrow 11$

Refinement

Refinement on F^2

Least-squares matrix: full

$R[F^2 > 2\sigma(F^2)] = 0.027$

$wR(F^2) = 0.077$

$S = 1.11$

1316 reflections

97 parameters

0 restraints

Primary atom site location: dual

Hydrogen site location: difference Fourier map

H-atom parameters constrained

$w = 1/[\sigma^2(F_o^2) + (0.0358P)^2 + 3.6714P]$

where $P = (F_o^2 + 2F_c^2)/3$

$(\Delta/\sigma)_{\max} < 0.001$

$\Delta\rho_{\max} = 0.90$ e Å⁻³

$\Delta\rho_{\min} = -0.51$ e Å⁻³

Special details

Geometry. All esds (except the esd in the dihedral angle between two l.s. planes) are estimated using the full covariance matrix. The cell esds are taken into account individually in the estimation of esds in distances, angles and torsion angles; correlations between esds in cell parameters are only used when they are defined by crystal symmetry. An approximate (isotropic) treatment of cell esds is used for estimating esds involving l.s. planes.

Fractional atomic coordinates and isotropic or equivalent isotropic displacement parameters (\AA^2)

	<i>x</i>	<i>y</i>	<i>z</i>	$U_{\text{iso}}^*/U_{\text{eq}}$
Mn	0.000000	0.21386 (5)	0.250000	0.01325 (16)
Al	0.16968 (5)	0.42298 (7)	0.07597 (8)	0.00506 (17)
P1	0.29135 (5)	0.62403 (6)	0.33188 (7)	0.00855 (16)
P2	0.000000	0.49748 (8)	0.250000	0.00678 (19)
N1	0.500000	0.3634 (4)	0.250000	0.0357 (10)
O1	0.20881 (14)	0.57892 (18)	0.1720 (2)	0.0129 (4)
O2	0.27155 (14)	0.77104 (18)	0.3420 (2)	0.0130 (4)
O3	0.27207 (14)	0.55150 (18)	0.4727 (2)	0.0132 (4)
O4	0.07105 (14)	0.40324 (18)	0.1938 (2)	0.0118 (4)
O5	0.06242 (14)	0.58669 (18)	0.3876 (2)	0.0116 (4)
O6	0.09702 (14)	0.09481 (19)	0.1661 (2)	0.0179 (4)
O7	0.11844 (17)	0.1969 (2)	0.4904 (3)	0.0262 (5)
H71	0.148203	0.266954	0.546232	0.039*
H72	0.160636	0.130057	0.499139	0.039*

Atomic displacement parameters (\AA^2)

	U^{11}	U^{22}	U^{33}	U^{12}	U^{13}	U^{23}
Mn	0.0131 (3)	0.0113 (3)	0.0168 (3)	0.000	0.0069 (2)	0.000
Al	0.0059 (3)	0.0047 (3)	0.0043 (3)	0.0007 (2)	0.0013 (3)	-0.0007 (2)
P1	0.0090 (3)	0.0086 (3)	0.0088 (3)	-0.0016 (2)	0.0039 (2)	-0.0006 (2)
P2	0.0071 (4)	0.0071 (4)	0.0063 (4)	0.000	0.0024 (3)	0.000
N1	0.041 (2)	0.0174 (19)	0.048 (3)	0.000	0.013 (2)	0.000
O1	0.0152 (9)	0.0132 (9)	0.0101 (8)	-0.0029 (7)	0.0039 (7)	-0.0037 (7)
O2	0.0168 (9)	0.0095 (9)	0.0137 (9)	-0.0030 (7)	0.0063 (7)	-0.0024 (7)
O3	0.0165 (9)	0.0124 (9)	0.0126 (9)	0.0010 (7)	0.0071 (7)	0.0029 (7)
O4	0.0125 (9)	0.0099 (8)	0.0153 (9)	0.0006 (7)	0.0078 (7)	0.0000 (7)
O5	0.0114 (8)	0.0123 (9)	0.0095 (8)	-0.0013 (7)	0.0010 (7)	-0.0036 (7)
O6	0.0107 (9)	0.0185 (10)	0.0265 (10)	-0.0019 (7)	0.0089 (8)	-0.0045 (8)
O7	0.0275 (12)	0.0201 (11)	0.0223 (10)	0.0016 (9)	-0.0040 (9)	-0.0044 (8)

Geometric parameters (\AA , $^\circ$)

Mn—O6	2.0799 (19)	Al—O4	1.9320 (18)
Mn—O6 ⁱ	2.0799 (19)	P1—O6 ^{iv}	1.5152 (19)
Mn—O7	2.199 (2)	P1—O2	1.5342 (19)
Mn—O7 ⁱ	2.199 (2)	P1—O3	1.5350 (18)
Mn—O4	2.2805 (18)	P1—O1	1.5493 (18)
Mn—O4 ⁱ	2.2805 (18)	P2—O5	1.5294 (18)

Mn—P2	2.9008 (10)	P2—O5 ⁱ	1.5294 (18)
Al—O2 ⁱⁱ	1.7847 (19)	P2—O4	1.5420 (18)
Al—O1	1.8013 (19)	P2—O4 ⁱ	1.5420 (18)
Al—O5 ⁱⁱⁱ	1.8080 (18)	O7—H71	0.8867
Al—O3 ⁱⁱⁱ	1.8886 (19)	O7—H72	0.8736
O6—Mn—O6 ⁱ	108.33 (11)	O5 ⁱⁱⁱ —Al—O4	90.54 (8)
O6—Mn—O7	87.58 (8)	O3 ⁱⁱⁱ —Al—O4	176.17 (8)
O6 ⁱ —Mn—O7	87.13 (8)	O6 ^{iv} —P1—O2	112.34 (11)
O6—Mn—O7 ⁱ	87.13 (8)	O6 ^{iv} —P1—O3	108.44 (11)
O6 ⁱ —Mn—O7 ⁱ	87.58 (8)	O2—P1—O3	110.49 (10)
O7—Mn—O7 ⁱ	170.96 (12)	O6 ^{iv} —P1—O1	111.15 (11)
O6—Mn—O4	93.99 (7)	O2—P1—O1	105.01 (10)
O6 ⁱ —Mn—O4	157.67 (7)	O3—P1—O1	109.38 (10)
O7—Mn—O4	93.15 (7)	O5—P2—O5 ⁱ	106.74 (14)
O7 ⁱ —Mn—O4	94.53 (7)	O5—P2—O4	113.09 (9)
O6—Mn—O4 ⁱ	157.67 (7)	O5 ⁱ —P2—O4	110.71 (9)
O6 ⁱ —Mn—O4 ⁱ	93.99 (7)	O5—P2—O4 ⁱ	110.71 (9)
O7—Mn—O4 ⁱ	94.53 (7)	O5 ⁱ —P2—O4 ⁱ	113.09 (9)
O7 ⁱ —Mn—O4 ⁱ	93.15 (7)	O4—P2—O4 ⁱ	102.63 (14)
O4—Mn—O4 ⁱ	63.72 (9)	O5—P2—Mn	126.63 (7)
O6—Mn—P2	125.84 (6)	O5 ⁱ —P2—Mn	126.63 (7)
O6 ⁱ —Mn—P2	125.84 (6)	O4—P2—Mn	51.31 (7)
O7—Mn—P2	94.52 (6)	O4 ⁱ —P2—Mn	51.31 (7)
O7 ⁱ —Mn—P2	94.52 (6)	P1—O1—Al	134.62 (12)
O4—Mn—P2	31.86 (4)	P1—O2—Al ^{iv}	144.61 (13)
O4 ⁱ —Mn—P2	31.86 (4)	P1—O3—Al ^v	131.12 (11)
O2 ⁱⁱ —Al—O1	123.95 (9)	P2—O4—Al	134.74 (11)
O2 ⁱⁱ —Al—O5 ⁱⁱⁱ	115.92 (9)	P2—O4—Mn	96.83 (9)
O1—Al—O5 ⁱⁱⁱ	120.10 (9)	Al—O4—Mn	127.51 (9)
O2 ⁱⁱ —Al—O3 ⁱⁱⁱ	91.29 (8)	P2—O5—Al ^v	139.42 (12)
O1—Al—O3 ⁱⁱⁱ	87.58 (8)	P1 ⁱⁱ —O6—Mn	127.16 (12)
O5 ⁱⁱⁱ —Al—O3 ⁱⁱⁱ	92.86 (8)	Mn—O7—H71	121.5
O2 ⁱⁱ —Al—O4	88.81 (8)	Mn—O7—H72	112.9
O1—Al—O4	89.19 (8)	H71—O7—H72	115.0

Symmetry codes: (i) $-x, y, -z+1/2$; (ii) $-x+1/2, y-1/2, -z+1/2$; (iii) $x, -y+1, z-1/2$; (iv) $-x+1/2, y+1/2, -z+1/2$; (v) $x, -y+1, z+1/2$.

Hydrogen-bond geometry ($\text{\AA}, ^\circ$)

$D-H\cdots A$	$D-H$	$H\cdots A$	$D\cdots A$	$D-H\cdots A$
O7—H71 ^v —O1 ^v	0.89	1.95	2.831 (3)	178
O7—H72 ^{vi} —O3 ^{vi}	0.87	2.04	2.897 (3)	166

Symmetry codes: (v) $x, -y+1, z+1/2$; (vi) $-x+1/2, -y+1/2, -z+1$.

Ammonium nickel(II) dialuminium tris(phosphate) dihydrate (II)

Crystal data

 $(\text{NH}_4)\text{NiAl}_2(\text{PO}_4)_3 \cdot 2\text{H}_2\text{O}$ $M_r = 451.65$ Monoclinic, $C2/c$ $a = 13.0711$ (3) Å $b = 10.1772$ (2) Å $c = 8.74476$ (19) Å $\beta = 108.527$ (3)° $V = 1103.00$ (4) Å³ $Z = 4$ $F(000) = 904$ $D_x = 2.720$ Mg m⁻³Mo $K\alpha$ radiation, $\lambda = 0.71073$ Å

Cell parameters from 14220 reflections

 $\theta = 2.6$ – 44.8 ° $\mu = 2.44$ mm⁻¹ $T = 298$ K

Plate, colourless

 $0.11 \times 0.04 \times 0.03$ mm

Data collection

XtaLAB Synergy, Single source at offset/far,

HyPix

diffractometer

Radiation source: micro-focus sealed X-ray

tube, PhotonJet (Mo) X-ray Source

Mirror monochromator

Detector resolution: 10.0000 pixels mm⁻¹ ω scans

Absorption correction: numerical

(CrysAlisPro; Rigaku OD, 2021)

 $T_{\min} = 0.853$, $T_{\max} = 0.962$

9320 measured reflections

1328 independent reflections

1281 reflections with $I > 2\sigma(I)$ $R_{\text{int}} = 0.021$ $\theta_{\max} = 28.0$ °, $\theta_{\min} = 2.6$ ° $h = -17 \rightarrow 17$ $k = -13 \rightarrow 13$ $l = -11 \rightarrow 11$

Refinement

Refinement on F^2

Least-squares matrix: full

 $R[F^2 > 2\sigma(F^2)] = 0.018$ $wR(F^2) = 0.056$ $S = 1.14$

1328 reflections

97 parameters

0 restraints

Primary atom site location: dual

Hydrogen site location: difference Fourier map

H-atom parameters constrained

 $w = 1/[\sigma^2(F_o^2) + (0.0245P)^2 + 3.4224P]$ where $P = (F_o^2 + 2F_c^2)/3$ $(\Delta/\sigma)_{\max} = 0.001$ $\Delta\rho_{\max} = 0.42$ e Å⁻³ $\Delta\rho_{\min} = -0.36$ e Å⁻³

Special details

Geometry. All esds (except the esd in the dihedral angle between two l.s. planes) are estimated using the full covariance matrix. The cell esds are taken into account individually in the estimation of esds in distances, angles and torsion angles; correlations between esds in cell parameters are only used when they are defined by crystal symmetry. An approximate (isotropic) treatment of cell esds is used for estimating esds involving l.s. planes.

Fractional atomic coordinates and isotropic or equivalent isotropic displacement parameters (Å²)

	<i>x</i>	<i>y</i>	<i>z</i>	$U_{\text{iso}}^*/U_{\text{eq}}$
Ni	0.000000	0.22315 (3)	0.250000	0.00786 (10)
Al	0.17218 (4)	0.42251 (5)	0.07491 (6)	0.00453 (12)
P1	0.29302 (4)	0.62530 (5)	0.32906 (5)	0.00592 (11)
P2	0.000000	0.49528 (6)	0.250000	0.00488 (13)
N1	0.500000	0.3647 (3)	0.250000	0.0282 (7)
O1	0.20866 (11)	0.57928 (13)	0.16956 (15)	0.0093 (3)
O2	0.26781 (11)	0.77156 (13)	0.34168 (16)	0.0091 (3)
O3	0.27630 (11)	0.54936 (13)	0.47120 (15)	0.0092 (3)
O4	0.07228 (11)	0.39900 (13)	0.19411 (16)	0.0085 (3)

O5	0.06302 (11)	0.58454 (13)	0.38790 (15)	0.0088 (3)
O6	0.09292 (11)	0.10007 (14)	0.17281 (17)	0.0119 (3)
O7	0.11014 (13)	0.20652 (15)	0.48072 (18)	0.0185 (3)
H71	0.147718	0.262282	0.538535	0.028*
H72	0.150318	0.137982	0.497836	0.028*

Atomic displacement parameters (Å²)

	U^{11}	U^{22}	U^{33}	U^{12}	U^{13}	U^{23}
Ni	0.00760 (16)	0.00725 (17)	0.00974 (17)	0.000	0.00416 (12)	0.000
Al	0.0051 (2)	0.0041 (2)	0.0044 (2)	0.00028 (18)	0.00137 (19)	0.00000 (17)
P1	0.0066 (2)	0.0055 (2)	0.0065 (2)	-0.00124 (15)	0.00321 (16)	-0.00082 (15)
P2	0.0047 (3)	0.0056 (3)	0.0045 (3)	0.000	0.0017 (2)	0.000
N1	0.0316 (16)	0.0160 (13)	0.0391 (17)	0.000	0.0143 (14)	0.000
O1	0.0120 (6)	0.0080 (6)	0.0078 (6)	-0.0016 (5)	0.0028 (5)	-0.0024 (5)
O2	0.0106 (6)	0.0065 (6)	0.0110 (6)	-0.0018 (5)	0.0044 (5)	-0.0021 (5)
O3	0.0111 (6)	0.0091 (6)	0.0090 (6)	0.0006 (5)	0.0056 (5)	0.0019 (5)
O4	0.0093 (6)	0.0073 (6)	0.0114 (6)	0.0005 (5)	0.0069 (5)	-0.0001 (5)
O5	0.0087 (6)	0.0097 (6)	0.0064 (6)	-0.0007 (5)	0.0002 (5)	-0.0020 (5)
O6	0.0085 (6)	0.0111 (6)	0.0183 (7)	-0.0002 (5)	0.0075 (5)	-0.0026 (5)
O7	0.0192 (8)	0.0153 (7)	0.0149 (7)	0.0010 (6)	-0.0032 (6)	-0.0033 (6)

Geometric parameters (Å, °)

Ni—O6	2.0052 (13)	Al—O4	1.9271 (14)
Ni—O6 ⁱ	2.0052 (13)	P1—O6 ^{iv}	1.5180 (14)
Ni—O7 ⁱ	2.0799 (15)	P1—O2	1.5361 (14)
Ni—O7	2.0799 (15)	P1—O3	1.5371 (13)
Ni—O4	2.1512 (13)	P1—O1	1.5502 (13)
Ni—O4 ⁱ	2.1513 (13)	P2—O5 ⁱ	1.5253 (13)
Ni—P2	2.7695 (7)	P2—O5	1.5253 (13)
Al—O2 ⁱⁱ	1.7731 (14)	P2—O4	1.5444 (13)
Al—O1	1.7908 (14)	P2—O4 ⁱ	1.5444 (13)
Al—O5 ⁱⁱⁱ	1.7979 (14)	O7—H71	0.8131
Al—O3 ⁱⁱⁱ	1.8818 (14)	O7—H72	0.8572
O6—Ni—O6 ⁱ	102.68 (8)	O5 ⁱⁱⁱ —Al—O4	90.50 (6)
O6—Ni—O7 ⁱ	85.94 (6)	O3 ⁱⁱⁱ —Al—O4	176.10 (6)
O6 ⁱ —Ni—O7 ⁱ	88.23 (6)	O6 ^{iv} —P1—O2	113.48 (8)
O6—Ni—O7	88.23 (6)	O6 ^{iv} —P1—O3	108.43 (8)
O6 ⁱ —Ni—O7	85.94 (6)	O2—P1—O3	109.89 (8)
O7 ⁱ —Ni—O7	170.66 (9)	O6 ^{iv} —P1—O1	111.07 (8)
O6—Ni—O4	94.96 (5)	O2—P1—O1	104.47 (8)
O6 ⁱ —Ni—O4	162.34 (5)	O3—P1—O1	109.41 (8)
O7 ⁱ —Ni—O4	93.78 (6)	O5 ⁱ —P2—O5	106.90 (11)
O7—Ni—O4	93.98 (6)	O5 ⁱ —P2—O4	111.02 (7)
O6—Ni—O4 ⁱ	162.34 (5)	O5—P2—O4	113.39 (7)
O6 ⁱ —Ni—O4 ⁱ	94.96 (5)	O5 ⁱ —P2—O4 ⁱ	113.39 (7)

O7 ⁱ —Ni—O4 ⁱ	93.98 (6)	O5—P2—O4 ⁱ	111.02 (7)
O7—Ni—O4 ⁱ	93.78 (6)	O4—P2—O4 ⁱ	101.24 (10)
O4—Ni—O4 ⁱ	67.41 (7)	O5 ⁱ —P2—Ni	126.55 (5)
O6—Ni—P2	128.66 (4)	O5—P2—Ni	126.55 (5)
O6 ⁱ —Ni—P2	128.66 (4)	O4—P2—Ni	50.62 (5)
O7 ⁱ —Ni—P2	94.67 (4)	O4 ⁱ —P2—Ni	50.62 (5)
O7—Ni—P2	94.67 (4)	P1—O1—Al	133.93 (9)
O4—Ni—P2	33.70 (3)	P1—O2—Al ^{iv}	142.39 (9)
O4 ⁱ —Ni—P2	33.71 (3)	P1—O3—Al ^v	128.58 (8)
O2 ⁱⁱ —Al—O1	124.32 (7)	P2—O4—Al	132.86 (8)
O2 ⁱⁱ —Al—O5 ⁱⁱⁱ	117.33 (7)	P2—O4—Ni	95.68 (6)
O1—Al—O5 ⁱⁱⁱ	118.28 (7)	Al—O4—Ni	130.40 (7)
O2 ⁱⁱ —Al—O3 ⁱⁱⁱ	92.12 (6)	P2—O5—Al ^v	140.21 (9)
O1—Al—O3 ⁱⁱⁱ	87.71 (6)	P1 ⁱⁱ —O6—Ni	126.87 (8)
O5 ⁱⁱⁱ —Al—O3 ⁱⁱⁱ	93.10 (6)	Ni—O7—H71	129.9
O2 ⁱⁱ —Al—O4	87.54 (6)	Ni—O7—H72	115.6
O1—Al—O4	89.27 (6)	H71—O7—H72	104.1

Symmetry codes: (i) $-x, y, -z+1/2$; (ii) $-x+1/2, y-1/2, -z+1/2$; (iii) $x, -y+1, z-1/2$; (iv) $-x+1/2, y+1/2, -z+1/2$; (v) $x, -y+1, z+1/2$.

Hydrogen-bond geometry ($\text{\AA}, ^\circ$)

$D-H\cdots A$	$D-H$	$H\cdots A$	$D\cdots A$	$D-H\cdots A$
O7—H71 \cdots O1 ^v	0.81	1.99	2.790 (2)	167
O7—H72 \cdots O3 ^{vi}	0.86	2.11	2.961 (2)	170

Symmetry codes: (v) $x, -y+1, z+1/2$; (vi) $-x+1/2, -y+1/2, -z+1$.